Research Article **Open Access**

Yuguang Jiang, Yu Feng, Silong Zhang, Jiang Qin*, and Wen Bao

Numerical heat transfer analysis of transcritical hydrocarbon fuel flow in a tube partially filled with porous media

DOI 10.1515/phys-2016-0073
Received Jul 19, 2016; accepted Oct 20, 2016

Abstract: Hydrocarbon fuel has been widely used in air-breathing scramjets and liquid rocket engines as coolant and propellant. However, possible heat transfer deterioration and threats from local high heat flux area in scramjet make heat transfer enhancement essential. In this work, 2-D steady numerical simulation was carried out to study different schemes of heat transfer enhancement based on a partially filled porous media in a tube. Both boundary and central layouts were analyzed and effects of gradient porous media were also compared. The results show that heat transfer in the transcritical area is enhanced at least 3 times with the current configuration compared to the clear tube. Besides, the proper use of gradient porous media also enhances the heat transfer compared to homogenous porous media, which could help to avoid possible over-temperature in the thermal protection.

Keywords: Heat transfer enhancement; Porous media; Metal foam; Hydrocarbon fuel; n-Decane

PACS: 44.30.+v

Nomenclature

C inertial resistance factor, m^{-1}
d tube diameter, m
e internal energy of fluid, $\frac{J}{kg}$
Gr Grashof number
h heat transfer coefficient, $\frac{W}{(m^2 \cdot K)}$
l_z the length of heated section, m
P pressure, Pa
P_b back pressure, Pa
q_w heat flux, $\frac{W}{m^2}$
Re Reynolds number
r radius coordinate, m
r_0 tube radius, m
r_p radius of porous media, m
T temperature, K
T_{in} inlet temperature, K
T_w wall temperature, K
$\overline{T_f}$ average fluid temperature, K
u axial velocity component, $\frac{m}{s}$
u_{in} inlet velocity, $\frac{m}{s}$
v radial velocity component, $\frac{m}{s}$
z axial coordinate, m

Greek Letters

α permeability of porous media, m^2
ϵ porosity
λ thermal conductivity, $\frac{W}{(m \cdot K)}$
λ_e effective thermal conductivity, $\frac{W}{(m \cdot K)}$
λ_f fluid thermal conductivity, $\frac{W}{(m \cdot K)}$
λ_s solid thermal conductivity, $\frac{W}{(m \cdot K)}$
μ viscosity, $Pa \bullet s$
ρ density, $\frac{kg}{m^3}$

Subscripts

w wall
f fluid
s solid
e effective

***Corresponding Author: Jiang Qin:** School of Energy Science and Engineering, Harbin Institute of Technology; Email: qinjiang@hit.edu.cn; Corresponding Address: No.92, West Da-Zhi Street, Harbin, Heilongjiang, 150001, P.R.China.
Yuguang Jiang, Yu Feng, Silong Zhang, Wen Bao: School of Energy Science and Engineering, Harbin Institute of Technology, China

1 Introduction

Thermal protection is one of the key issues when developing both air-breathing and rocket engines, especially in a scramjet [1–3]. The thermal load is extremely large due to a high combustion temperature and high flight Mach number. Due to the high total temperature of free stream, air cannot be used as the coolant anymore as in the traditional engines. Regenerative cooling using endothermic hydrocarbon fuel has been considered as the most promising cooling method for the scramjet [4, 5, 7, 8]. Fuel flows through the wall to cool it down before it's injected into the combustor. The heat transfer efficiency has thus become the key factor affecting the thermal protection. However, dramatic changes in properties when hydrocarbon fuel experiences the pseudo-critical temperature during the cooling [9] may lead to severe heat transfer deterioration [10–13] and the structure may get over-temperature, which is unacceptable. For another, at a certain local high heat flux zone, for example, the cavity, heat flux can be as high as $3MW/m^2$, which is a serious challenge for thermal protection [14, 15]. As a result, proper heat transfer enhancement methods for hydrocarbon fuel are in urgent need.

Heat transfer enhancement has been one of the research focuses in all kinds of heat exchangers [16], since it is efficient in boosting the operation economy and keeping the temperature of heat sources normal. Increasing the heat exchange area and surface heat transfer coefficient have been proved to be valid rules for heat transfer enhancement. The local structures, such as ribs, grooves and rough surfaces, are classic examples of these two rules [17]. More than that, it's worth noting that the porous medium has shown an excellent capability in heat transfer enhancement. The porous medium contains a tremendous specific surface area since its loose and porous internal structure, raises the heat exchange area greatly. What's more, the effective thermal conductivity can be highly enhanced by a porous medium like metal foam [18]. Thus, heat transfer enhancement using a porous medium has drawn wide and consistent research interests.

Moran Wang investigated the effective conductivity of high porosity porous foam using the lattice boltzmann method considering the radiation effect [19], and the effective physical properties of complex multiphase materials were also studied [20]. K. Vafai1 and S. J. Kim developed a theoretical model for heat transfer in a porous medium and found the thickness of the momentum boundary layer depends on both the Darcy number and the inertia parameter for a high permeability [21]. AA. Mohamad found similar results with a two dimensional model and the best porous radius ratio was discussed [22]. M.E. Nimvari *et al.* studied both central and boundary arrangements and the results show that porous thickness depends on Da number much less in turbulence than in laminar flow [23]. M.K. Alkam *et al.* researched the heat transfer in parallel plates with porous inserts and the effects of thermal conduction ratio, Darcy number, and microscopic inertial coefficient were presented [24]. A local thermal non-equilibrium model is another research interest [25–27]. Besides, there is experimental research about heat transfer of air or water in ducts or channels with porous inserts or ribs [28–31].

So far, adjusting the aspect ratios [32–34] and use of ribs [35] are common methods to enhance the heat transfer of hydrocarbon fuel. Gascoin and his team have published work about the permeation, pyrolysis and coke formation of high temperature hydrocarbon fuel in a porous medium like metal foam [36–38]. However, the heat transfer enhancement is not the focus. Research on heat transfer enhancement of hydrocarbon fuel using a porous medium is hardly found. Fortunately, cooling channels of a scramjet are not that sensitive to the extra pressure drop caused by a porous media as flow restrictions are essential to keep a supercritical pressure and to adjust the fuel supply, which makes the porous media a potential method for heat transfer enhancement of hydrocarbon fuel in applications like scramjets.

In this work, a 2-D numerical model was developed to investigate the heat transfer enhancement of hydrocarbon fuel in a tube partially filled by metal foam under supercritical pressure. Different schemes of heat transfer enhancement were studied and compared. The characteristics of heat transfer enhancement were presented.

2 Model descriptions

2.1 Physical model

Tubes are usually used to simulate the cooling channels of scramjet. A 2-D steady state and axisymmetric numerical model using commercial CFD code, Ansys/Fluent, was established in this work, as illustrated in Fig. 1 (L_2 = 100 mm, r_p = 0.75 mm). Three arrangements were presented which respectively are (a). boundary arrangement, (b). the central arrangement and (c). the boundary fin for the comparison reason.

N-Decane is selected as the fluid. The tube is made of steel. There is an entrance section and exit section before/after the heated flow passage. The porous medium is steel foam (ϵ = 0.876 and PPI = 20 for the homogenous

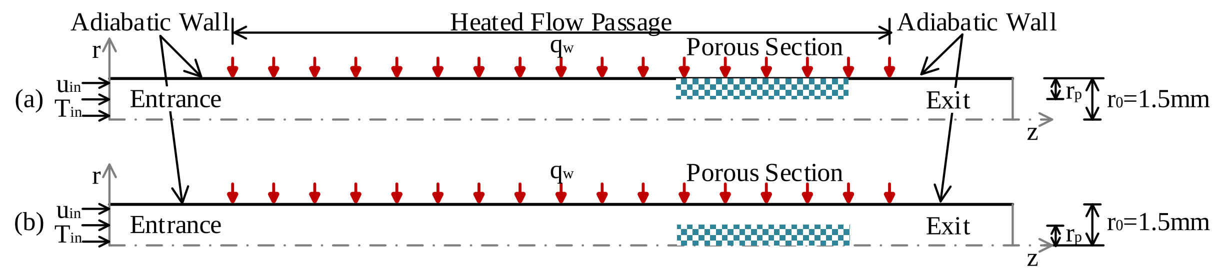

Figure 1: Schematic of the problem.

cases) partially placed parallel to the central line of the tube in the boundary or the core.

2.2 Governing equations

A local thermal equilibrium (LTE) assumption is usually assumed to exist between solid and fluid phase when the volumetric heat transfer coefficient is high and there is no heat released in the fluid or solid phase [39, 40]. Therefore, LTE is assumed in our work. As regards the common used turbulence model, the $k-\epsilon$model is applicable to free-shear-layer flows with small pressure gradients [41]. The $k-\omega$model goes for flows with adverse pressure gradients and separation [42–44]. Considering the high heat flux and dramatic thermos-physical property variation in the near wall region as well as the low-Re turbulent flow in this work, the *SST* $k-\omega$turbulence model is adopted [45]. The buoyancy effect is neglected as $\frac{Gr}{Re^2} \ll 1$. The SIMPLEC algorithm was adopted. The continuity, momentum and energy equations are listed below,

Continuity Equation

$$\frac{1}{r}\frac{\partial(\rho ur)}{\partial r}+\frac{\partial(\rho u)}{\partial z}=0 \quad (1)$$

r-Momentum Equation

$$\frac{1}{r}\frac{\partial(\rho vvr)}{\partial r}+\frac{\partial(\rho vu)}{\partial z}=-\frac{\partial P}{\partial r}+\frac{1}{r}\frac{\partial}{\partial r}\left(r\mu\frac{\partial v}{\partial r}\right) + \frac{\partial}{\partial z}\left(\mu\frac{\partial v}{\partial z}\right)-\mu\frac{v}{r^2}-f(\frac{\mu}{\alpha}v+C\frac{1}{2}\rho\,|V|\,v) \quad (2)$$

z-Momentum Equation

$$\frac{\partial(\rho uu)}{\partial z}+\frac{1}{r}\frac{\partial(\rho uvr)}{\partial r}=-\frac{\partial P}{\partial z}+\frac{1}{r}\frac{\partial}{\partial r}\left(r\mu\frac{\partial u}{\partial r}\right) + \frac{\partial}{\partial z}\left(\mu\frac{\partial u}{\partial z}\right)-f(\frac{\mu}{\alpha}u+C\frac{1}{2}\rho\,|V|\,u) \quad (3)$$

The parameter f is set to unity for the porous region and zero for the clear region $|V| = \sqrt{u^2+v^2}$.

Energy Equation (The viscous dissipation and heat generation is neglected)

$$\frac{\partial(\rho eu)}{\partial z}+\frac{1}{r}\frac{\partial(\rho erv)}{\partial r}=\lambda_e\frac{\partial}{\partial z}\left(\frac{\partial T}{\partial z}\right)+\frac{1}{r}\frac{\partial}{\partial r}\left(r\frac{\partial T}{\partial r}\right) \quad (4)$$

The Peng-Robinson equation of state is used in this paper to predict the density of fluid in a wide range (from liquid to gas) [5] with a good prediction of the fuel properties near the critical points [6]. It requires knowing the critical properties such as the critical temperature, pressure, volume and the acentric factor. In the porous zone, the physical properties are obtained by combining properly the fluid characteristics with the solid ones. For example, by default, λ_e is the effective thermal conductivity of fluid plus solid evaluated with a parallel law. Pyrolysis is not considered for this work and the fuel temperature is set lower than its pyrolysis point [46].

$$\lambda_e=\epsilon\lambda_f+(1-\epsilon)\lambda_s \quad (5)$$

The heat transfer coefficient is calculated as follows

$$h=\frac{q_w}{(t_w-t_f)} \quad (6)$$

2.3 Boundary conditions

Asymmetric boundary is set at $r = 0$.

Inlet boundary conditions:

$$u=u_{in},\ v=0,\ T=T_{in} \quad (7)$$

Wall boundary conditions:

The wall of entrance and exit section is set as adiabatic, and constant heat flux is set on the wall of the heated flow passage. No slip boundary condition is defined for the wall.

The adiabatic wall

$$u=0,\ v=0,\ \frac{\partial T}{\partial r}=0 \quad (8)$$

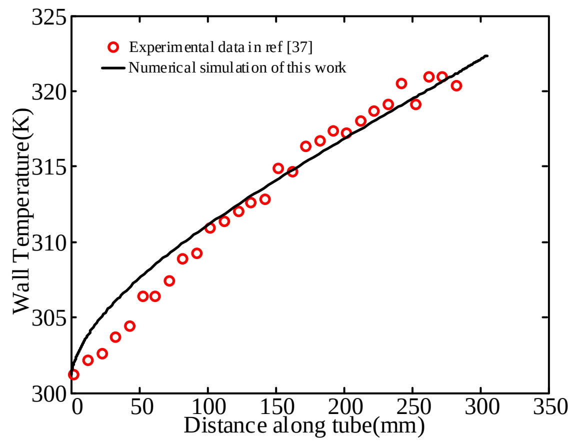

Figure 2: Comparison of wall temperature between this study and Nihad Dukhan *et al's* [47].

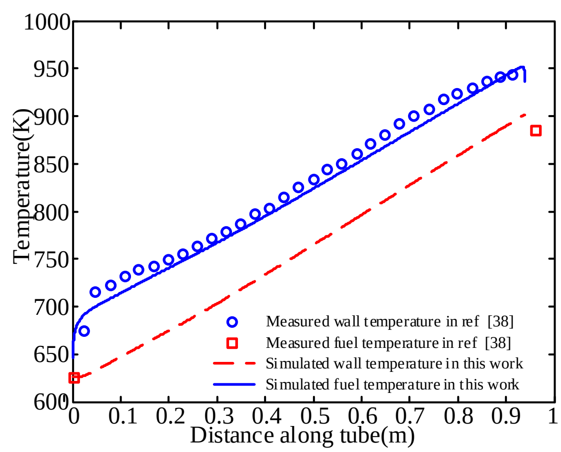

Figure 3: Comparison of wall temperature and fuel temperature between this study and Jiang's [48].

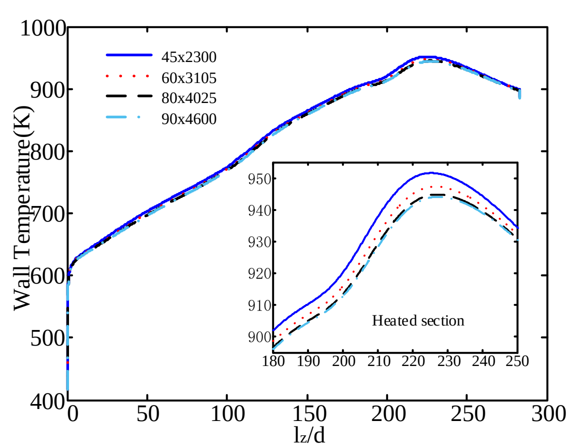

Figure 4: Grid independent test of wall temperature for clear tube.

The heated wall with constant heat flux

$$u = 0,\ v = 0, -\lambda \frac{\partial T}{\partial r} = q_w \tag{9}$$

The inlet temperature is 400 K and mass flow rate is 8 g/s. The inlet Reynold number is 11275 to ensure a pure turbulence flow. The outlet backpressure P_b is set to be 3 MPa which is supercritical for n-Decane.

3 Validations

3.1 Model validation

In order to verify the numerical solution of fluid flow and heat transfer inside the porous media, the geometry and boundary conditions of Nihad Dukhan *et al's* experiments [47] has been simulated. The pipe is fully filled with aluminum foam. Fig. 2 shows the simulation of wall temperature of this study and experiment in [47]. Good agreement is found between this simulation and the experiment.

In addition, the description of flow and heat transfer of n-Decane under supercritical pressure is also validated. Numerical study with the geometry and boundary conditions of Jiang's study [48] was carried out. Since pyrolysis conversion rate is less than 10% according to the experimental data, the pyrolysis was neglected in the simulation. Fig. 3 shows the wall and fuel temperature of this simulation and experiment data. Good agreement is found between this simulation and the experiment.

3.2 Grid independence analysis

Different mesh sizes 45 × 2300, 60 × 3150, 80 × 4250, 90 × 4600 were compared to test the model. The solution is considered to be converged when the normalized residual of the algebraic equation is less than a prescribed value of 10^{-6}. The analysis below will only focus on the heated section and the z-coordinates are presented by $\frac{l_z}{d}$. As shown in Fig. 4 and Fig. 5, the 80 × 4025 size grid was used because the difference in T_w is less than 0.0976% and the difference in $h$is less than 0.35% when compared with the mesh 90 × 4600 (h is high at the start of heated section since thermal boundary layer has not established. It's not shown in full scale for the convenience of view.)

4 Results and Discussion

Regenerative cooling using hydrocarbon fuel has been considered to be the most promising cooling method for a scramjet. However, heat transfer deterioration may hap-

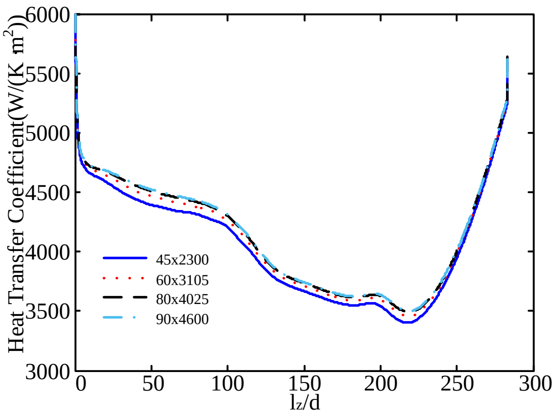

Figure 5: Grid independent test of heat transfer coefficient for clear tube.

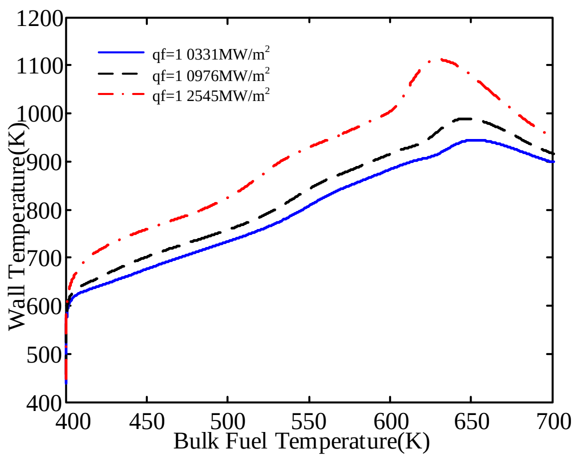

Figure 6: Heat transfer deterioration with different heat flux.

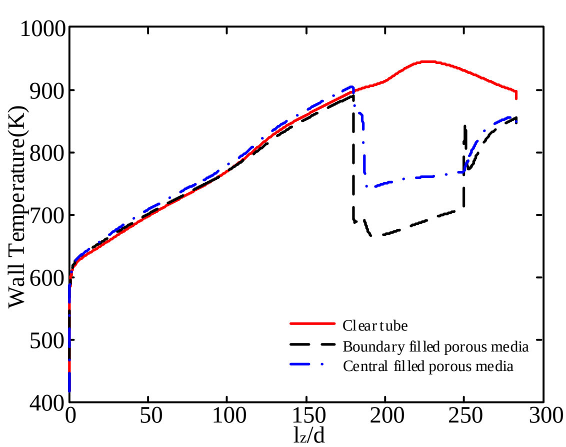

Figure 7: Wall temperature of clear tube and porous media layouts.

pen because of the transcritical process. As shown in Fig. 6, the length of heated zone varies from 700 mm to 850 mm to achieve different heat flux and the same fuel

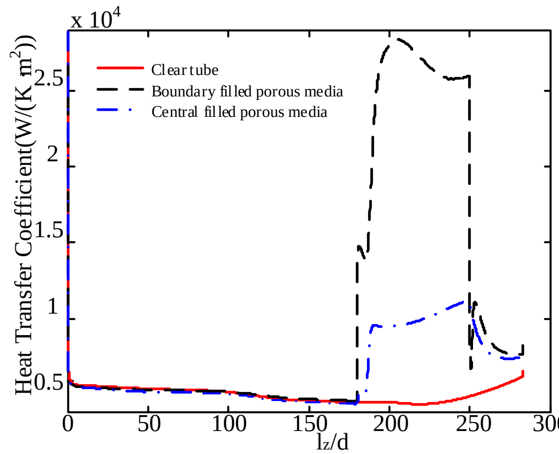

Figure 8: Heat transfer coefficient of clear tube and porous media layouts.

temperature in outlet. Heat transfer deterioration occurs and worsen with higher heat flux. The properties of hydrocarbon fuel vary with temperature dramatically, which affects the heat transfer in turn. To make it clear for analysis, the pseudo-critical temperature zone is chosen in this work. Steel foam is used as the porous media and set in this zone as illustrated in Fig. 1. The thermal conductivity is temperature dependent. $q_w = 1.0331\frac{MW}{m^2}$ is set for all the following cases.

4.1 Effect of homogenous porous media

The wall temperature and heat transfer coefficient are shown in Fig. 7 and Fig. 8 respectively. The heat transfer is enhanced in the porous section in both layouts and the wall temperature falls obviously compared to the clear tube. Porous media increases the heat exchange area greatly. Besides, as illustrated by Eq. 8, the effective thermal conductivity is much larger than the pure n-Decane. Especially in the boundary layout, there is direct contact between the porous media and the wall and the heat transfer is thus enhanced 6-7. 76 times in heat transfer coefficient. Considering the assumption LTE, the result maybe a little optimistic. Still, the heat transfer is enhanced about 3 times in central scheme, which proved the effect of a porous media. Meanwhile, as shown in Fig. 9, the turbulence kinetic energy increases due to the flow disturbance of the porous media. Velocity rises in the clear region of boundary layout and larger velocity gradient enhances the heat transfer, too.

Besides, slight heat transfer deterioration occurs in the start of porous zone. As shown in Fig. 7, the heat trans-

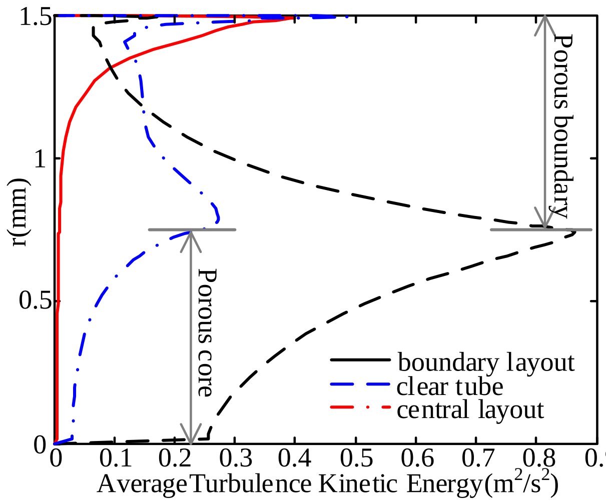

Figure 9: Turbulence kinetic energy of clear tube and porous media layouts.

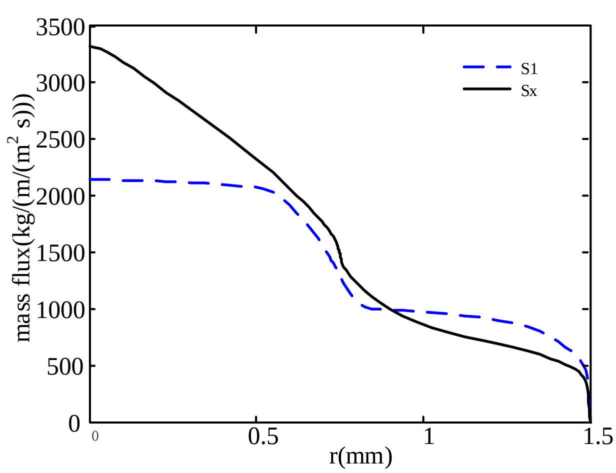

Figure 10: The mass flux of S1 and Sx.

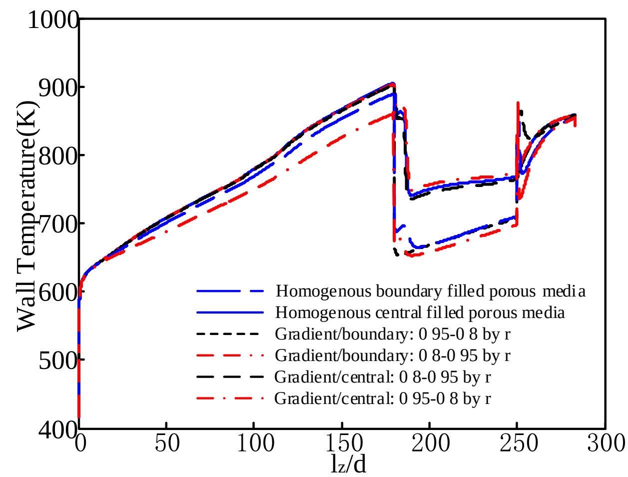

Figure 11: Wall temperature of gradient porous media layouts.

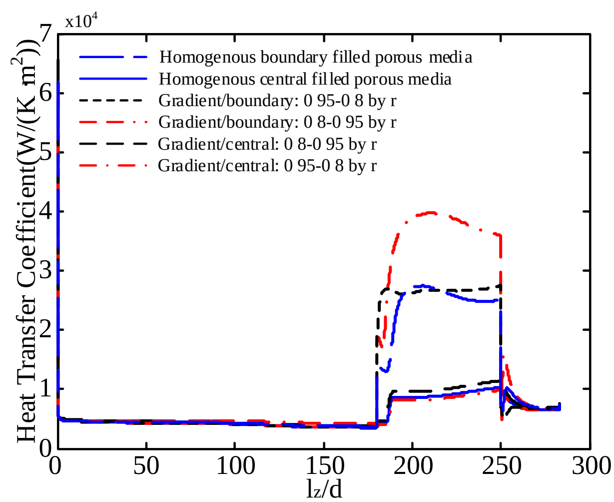

Figure 12: Heat transfer coefficient of gradient porous media.

fer deterioration point is defined as Sx and the peak in h before is defined as S1. Mass averaged temperature of the deterioration area is around the critical temperature 617.7K. Sharp variation of properties occurs. The ρu distribution of S1 and Sx are demonstrated in Fig. 10. It can be seen that ρu is much lower in Sx due to the sharp density decrease of n-Decane in the transcritical temperature. Local heat transfer deteriorates as the fluid is less concentrated here. The heat transfer deterioration after the porous media zone is mainly because of the local vortex zone caused by the geometry layout.

In the central layout, high effective thermal conductivity helps to transfer the heat to the central part of the fluid, too. Yet, there is no direct contact with the wall, and increase of turbulence kinetic energy in the boundary part becomes the main reason of heat transfer enhancement (shown in Fig. 9).

As mentioned above, the r_p of boundary and central layouts are both 0.5. However, the flow area of clear region in boundary layout is only 1/3 of central layout, which leads to a higher turbulence kinetic energy in boundary layout. Besides, there's no direct contact between porous media and wall in the central layout. Thus the effect of increase in effective thermal conductivity is weakened. As a result, the heat transfer is better enhanced with boundary filled with porous media.

Accordingly, the pressure drop is higher in boundary layout since there is a smaller clear region area, as can be seen in Table 1. Nevertheless, it's a partial fill and only for a short length, the pressure drop increase is not that obvious when compared to the critical pressure of hydrocar-

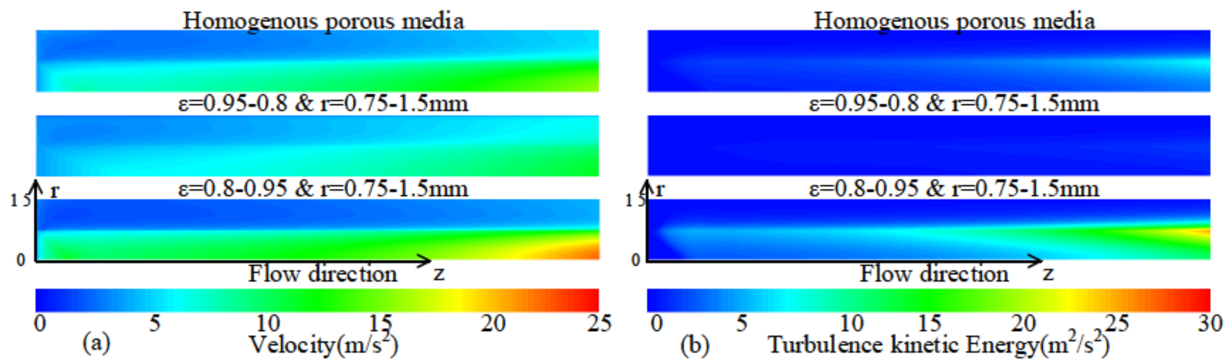

Figure 13: The velocity and turbulence kinetic energy of gradient porous boundary layouts.

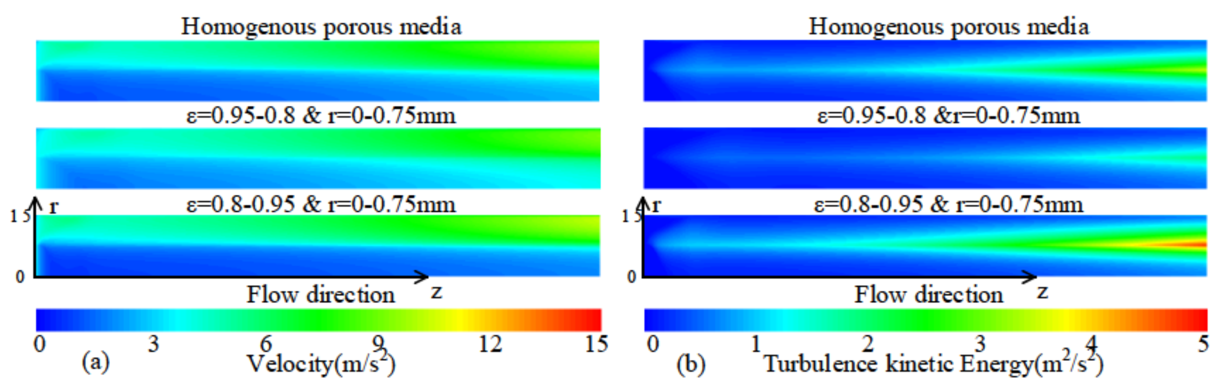

Figure 14: The velocity and turbulence kinetic energy of gradient porous central layouts.

Table 1: Pressure drop of heated section in different layouts.

Layouts	Pressure drop of heated section (kPa)
Clear tube	15.35
Boundary filled	173.78
Central filled	45.289

bon fuel. As stated earlier, cooling channels of a scramjet are not that sensitive to pressure drop as the supercritical pressure is usually maintained to avoid the boiling heat transfer deterioration.

4.2 Effect of gradient porous media

The gradient porous media is a good way to adjust the heat transfer effect without changing the fill ratio, which gives more degree of freedom. In this section, gradient porous media in two layouts were simulated and analyzed. Porosity is assumed to distributed from 0.8 to 0.95 by r linearly or in reverse and homogenous in the z direction. Here we call the porous media positive gradient when $\frac{d\epsilon}{dr} > 0$; otherwise, the negative gradient.

As presented in Fig. 11 and Fig. 12, it can be seen that the gradient porous media functions differently in boundary and central filled layouts. In boundary filled layout, positive gradient porous media enhances the heat transfer better and h increases by about 40%. From the perspective of velocity and turbulence kinetic energy, it can be explained as follows. Positive gradient means lower porosity adjacent to the clear region and decreases the effective flow area in reality. As a result, in Fig. 13 it's seen that the velocity in the clear region is higher and so is the turbulence kinetic energy. Positive gradient intensifies the turbulence of clear region and in turn reinforces the heat transfer. As to the negative gradient, velocity in clear region drops a little and turbulence kinetic energy is lower too. The heat transfer is only slightly changed compared with the homogenous porous condition.

In the central filled layout, positive gradient also enhances the heat transfer. But unlike the boundary layout, positive gradient means higher porosity adjacent to the clear region. As we can see in Fig. 14(a), the velocity field is almost the same. The main effect of gradient porous media is the increase of the turbulence kinetic energy shown in Fig. 14(b). Therefore, the heat transfer is enhanced by about 10% increase in h. This is concluded in a turbulence flow. However, it's different in a laminar flow as presented in Wang *et al's* work [39]. Without turbulence, velocity variation due to the change of effective area becomes the key factor. Positive gradient means the higher porosity area is adjacent to the clear region, which leads to larger flow area and lower velocity. The heat transfer thus deteriorates. The results are accordant with conclusion of this work.

5 Conclusions

In this work, a 2-D steady numerical simulation is carried out to investigate the heat transfer in a porous media partially filled tube with hydrocarbon fuel under supercritical pressure. The effects of homogenous and gradient porous media were both studied. The layouts of boundary and central filled were compared. All the simulations were performed with $r_p = 0.5$. The results show that:

1. Heat transfer is enhanced with porous media partially filled. The kinetic turbulence energy is higher in global aspect and velocity in the clear region rises to make a larger velocity gradient, which both contribute to the heat transfer enhancement.
2. The effect of boundary layout with homogenous porous media is better (the h increases to 6-7.76 times) with $r_p = 0.5$, while h increases about 3 times in the central scheme. This is because the effective thermal conductivity of porous zone contributes to the convection with wall directly.
3. In boundary layout, a gradient porous media with lower porosity adjacent to clear region enhances the heat transfer by 40% increase in h; as it decreases the flow area and increases the velocity in clear region. Thus, the turbulence is strengthened and heat transfer is enhanced.
4. However, in central layout, heat transfer is enhanced by gradient porous media with higher porosity adjacent to clear region by 10% increase in h. Since the change in flow area is not obvious while the flow is disturbed and the turbulence kinetic energy increases; the heat transfer is thus enhanced

Generally, heat transfer enhancement using a porous media is valid, but more parametric study is needed, which is also the future research focus.

Acknowledgement: This work was supported by General Program (No. 51476044), General Program (No. 51276047) and Innovative Research Groups (No. 51421063) of National Natural Science Foundation of China, and the authors thank the reviewers for their valuable advice on this paper.

References

[1] Curran E T. Scramjet engines: the first forty years[J]. Journal of Propulsion and Power, 2001, 17(6):1138-1148
[2] Qin J, Bao W, Zhang S L, *et al.* Thermodynamic analysis for a chemically recuperated scramjet[J]. Science China Technological Sciences, 2012, 11(11):3204-3212.
[3] Zhang S L, Qin J, Bao W, *et al.* Thermal management of fuel in advanced aeroengine in view of chemical recuperation[J]. Energy. 2014,77: 201-211.
[4] Feng Y, Qin J, Bao W, *et al.* Modeling and analysis of heat and mass transfers of supercritical hydrocarbon fuel with cracking in mini-channel[J]. International Journal of Heat and Mass Transfer. 2015, 91:520-531.
[5] Bao W, Zhang S L, Qin J, *et al.* Numerical analysis of flowing cracked hydrocarbon fuel inside cooling channels in view of thermal management[J]. Energy. 2014,67:149-161.
[6] Peng D. Y., Robinsion D. B.. "A new two-constant equation of state," Industrial & Engineering Chemistry Fundamentals, Vol. 51, No. 1, 1976, pp.59-64.
[7] Jiang Y G, Zhang S L, Feng Y, *et al.* A control method for flow rate distribution of cracked hydrocarbon fuel in parallel channels[J]. Applied Thermal Engineering. 2016,doi:10.1016/j.applthermaleng.2016.03.031.
[8] Qin J, Zhang S L, Bao W, *et al.* Thermal management method of fuel in advanced aeroengines[J]. Energy. 2013, 49(1): 459-468.
[9] Qin J, Jiang Y G, Feng Y, *et al.* Flow rate distribution of cracked hydrocarbon fuel in parallel pipes[J]. Fuel. 2015,161:105-112.
[10] Wang Y H, Li S F, Dong M. Numerical study on heat transfer deterioration of supercritical n-Decane in horizontal circular tubes[J]. Energies. 2014,7: 7535-7554; doi:10.3390/en7117535
[11] Liu B, Zhu Y H, Yan J J, *et al.* Experimental investigation of convection heat transfer of n-Decane at supercritical pressures in small vertical tubes[J]. International Journal of Heat and Mass Transfer. 2015; 91: 734–746.
[12] Li W, Huang D, Xu G Q, *et al.* Heat transfer to aviation kerosene flowing upward in smooth tubes at supercritical pressures[J]. International Journal of Heat and Mass Transfer. 2015; 85: 1084–1094.
[13] Zhu J Q, Tao Z, Deng H W, *et al.* Numerical investigation of heat transfer characteristics and flow resistance of kerosene RP-3 under supercritical pressure[J]. International Journal of Heat and Mass Transfer. 2015; 91: 330–341.
[14] Powell O A, Edwards J T, Norris R B, *et al.* Development of hydrocarbon-fueled scramjet engines: the hypersonic technology (HyTech) Program[J]. Journal of Propulsion and Power, 2001, 17(6): 1170-1176.
[15] Song K D, Choi S H, Scotti S J. Transpiration cooling experiment for scramjet engine combustion chamber by high heat fluxes[J].

Journal of propulsion and Power, 2006, 22(1): 96-102.

[16] Bergles A E. ExHFT for fourth generation heat transfer technology[J]. Experimental Thermal and Fluid Science, 2002, 26(2): 335-344.

[17] Webb R L, Eckert E R G, Goldstein R J. Heat transfer and friction in tubes with repeated-rib roughness[J]. International Journal of Heat and Mass Transfer, 1971, 14(4): 601-617.

[18] Zheng Z J, Li J M, He Y L. Optimization of porous insert configurations for heat transfer enhancement in tubes based on genetic algorithm and CFD[J]. International Journal of Heat and Mass Transfer, 2015; 87: 376-379.

[19] Wang M, Pan N. Modeling and prediction of the effective thermal conductivity of random open-cell porous foams[J]. International Journal of Heat & Mass Transfer, 2008, 51(5–6):1325-1331.

[20] Wang M, Pan N. Predictions of effective physical properties of complex multiphase materials[J]. Materials Science & Engineering R Reports, 2008, 63(1):1-30.

[21] Vafai KK, Kim SJ. Forced convection in a channel filled with a porous medium: an exact solution [J]. ASME. J. Heat Transfer. 1989;111(4):1103-1106. doi:10.1115/1.3250779.

[22] Mohamad A A. Heat transfer enhancements in heat exchangers fitted with porous media Part I: constant wall temperature[J]. International Journal of Thermal Sciences, 2003, 42(4):385-395.

[23] Nimvari M E, Maerefat M, El-Hossaini M K. Numerical simulation of turbulent flow and heat transfer in a channel partially filled with a porous media[J]. International Journal of Thermal Sciences, 2012, 60(1):131-141.

[24] Alkam M K, Al-Nimr M A, Hamdan M O. Enhancing heat transfer in parallel-plate channels by using porous inserts[J]. International Journal of Heat and Mass Transfer, 2001, 44(5):931-938.

[25] Mahmoudi Y, Karimi N. Numerical investigation of heat transfer enhancement in a pipe partially filled with a porous material under local thermal non-equilibrium condition[J]. International Journal of Heat and Mass Transfer, 2014, 68(1):161-173.

[26] Mahmoudi Y, Karimi N, Mazaheri K. Analytical investigation of heat transfer enhancement in a channel partially filled with a porous material under local thermal non-equilibrium condition[J]. International Journal of Heat and Mass Transfer, 2014, 70: 875–891

[27] Zhang L, Luo F, Xu R N, *et al.* Heat transfer and fluid transport of supercritical CO2 in enhanced geothermal system with local thermal non-equilibrium model[J]. Energy Procedia, 2014, 63(2):7644-7650.

[28] Hamadouche A, Nebbali R, Benhamed H, *et al.* Experimental investigation of convective heat transfer in an open-cell aluminum foams[J]. Experimental Thermal and Fluid Science, 2016, 71:86-94.

[29] Jeng T M, Tzeng S C, Lin Y C. Experimental study of heat transfer enhancement of inserted LED lamp by the closed-cell aluminum-foam ceiling[J]. International Communications in Heat and Mass Transfer, 2015, 66:233–239.

[30] Calmidi V V, Mahajan R L. Forced convection in high porosity metal foams[J]. Journal of Heat Transfer, 2000, 122(3):557-565.

[31] Dukhan N, Özer Bağcı, Özdemir M. Thermal development in open-cell metal foam: an experiment with constant wall heat flux[J]. International Journal of Heat and Mass Transfer, 2015, 85:852-859.

[32] Xu K, Bo R, Meng H. A thermal performance factor for evaluation of active engine cooling with asymmetric heating[J]. Applied Thermal Engineering, 2014, 73(1):351-356.

[33] Pizzarelli M, Nasuti F, Onofri M. Flow Analysis of Transcritical Methane in Rectangular Cooling Channels[C]// Aiaa/asme/sae/asee Joint Propulsion Conference & Exhibit. 2008.

[34] Ulas A, Boysan E. Numerical analysis of regenerative cooling in liquid propellant rocket engines[J]. Aerospace Science & Technology, 2013, 24(1):187-197.

[35] Xu K, Tang L, Meng H. Numerical study of supercritical-pressure fluid flows and heat transfer of methane in ribbed cooling tubes[J]. International Journal of Heat & Mass Transfer, 2015, 84:346-358.

[36] Gascoin N. High temperature and pressure reactive flows through porous media[J]. International Journal of Multiphase Flow. 2011; 37:24-35.

[37] Gascoin N, Romagnosi L, Fedioun I, *et al.* Pyrolysis in porous media: part 2. numerical analysis and comparison to experiments[J]. Journal of Porous Media. 2013; 16(9): 857-873.

[38] Fan G, Gascoin N, Gillard P, *et al.* Fuel pyrolysis through porous media: Coke formation and coupled effect on permeability[J]. Journal of Analytical and Applied Pyrolysis. 2012; 95:180-188.

[39] Wang B, Hong Y, Hou X, *et al.* Numerical configuration design and investigation of heat transfer enhancement in pipes filled with gradient porous materials[J]. Energy Conversion & Management, 2015, 105:206-215.

[40] Yang Y T, Hwang M L. Numerical simulation of turbulent fluid flow and heat transfer characteristics in heat exchangers fitted with porous media[J]. International Journal of Heat & Mass Transfer, 2009, 52(13–14):2956-2965.

[41] Bardina J E, Huang P G, Coakley T J. Turbulence Modeling Validation, Testing, and Development[R]. California US, Ames Research Center, 1997.

[42] Huang W, Liu W D, Li S, *et al.* Influences of the turbulence model and the slot width on the transverse slot injection flow field in supersonic flows[J]. Acta Astronautica, 2012, 73(2):1-9.

[43] Huang W, Li S, Yan L, *et al.* Performance evaluation and parametric analysis on cantilevered ramp injector in supersonic flows[J]. Acta Astronautica, 2013, 84(3):141-152.

[44] Huang W. Design exploration of three-dimensional transverse jet in a supersonic crossflow based on data mining and multi-objective design optimization approaches[J]. International Journal of Hydrogen Energy, 2014, 39(8):3914-3925.

[45] Hua Y X, Wang Y Z, Meng H. A numerical study of supercritical forced convective heat transfer of n-heptane inside a horizontal miniature tube[J]. Journal of Supercritical Fluids the, 2010, 52(1):36-46.

[46] Zhou W, Jia Z, Qin J, *et al.* Experimental study on effect of pressure on heat sink of n-Decane[J]. Chemical Engineering Journal, 2014, 243(4):127-136.

[47] Dukhan N, Özer Bağcı, Özdemir M. Thermal development in open-cell metal foam: An experiment with constant wall heat flux[J]. International Journal of Heat & Mass Transfer, 2015, 85:852-859.

[48] Zhu Y, Liu B, Jiang P. Experimental and Numerical Investigations on n-Decane Thermal Cracking at Supercritical Pressures in a Vertical Tube[J]. Energy & Fuels, 2013, 28(1):2187–2193.